HAT-P-6b: A HOT JUPITER TRANSITING A BRIGHT F STAR †

R. W. Noyes¹, G. Á. Bakos^{1,2}, G. Torres¹, A. Pál^{1,3}, Géza Kovács⁴, D. W. Latham¹, J. M. Fernández¹, D. A. Fischer⁵, R. P. Butler⁶, G. W. Marcy⁷, B. Sipőcz^{3,1}, G. A. Esquerdo¹, Gábor Kovács¹, D. D. Sasselov¹, B. Sato⁸, R. Stefanik¹, M. Holman¹, J. Lázár⁹, I. Papp⁹ & P. Sári⁹

Draft version October 24, 2018 – VERSION 14

ABSTRACT

In the ongoing HATNet survey we have detected a giant planet, with radius $1.33\pm0.06~R_{\rm Jup}$ and mass $1.06\pm0.12~M_{\rm Jup}$, transiting the bright (V=10.5) star GSC 03239-00992. The planet is in a circular orbit with period $3.852985\pm0.000005\,{\rm days}$ and mid-transit epoch $2.454,035.67575\pm0.00028\,{\rm (HJD)}$. The parent star is a late F star with mass $1.29\pm0.06~M_{\odot}$, radius $1.46\pm0.06~R_{\odot}$, $T_{\rm eff}\sim6570\pm80\,{\rm K}$, $[{\rm Fe/H}]=-0.13\pm0.08$ and age $\sim2.3^{+0.5}_{-0.7}\,{\rm Gy}$. With this radius and mass, HAT-P-6b has somewhat larger radius than theoretically expected. We describe the observations and their analysis to determine physical properties of the HAT-P-6 system, and briefly discuss some implications of this finding. Subject headings: stars: individual (GSC 03239-00992, HAT-P-6) – planetary systems

1. INTRODUCTION

The detection of transiting exoplanets is very important to exoplanet research because of the information about both planetary radius and mass that comes from photometric transit light curves combined with followup radial velocity observations. The transiting exoplanets known as of this writing span a wide range in the physical parameter space of planetary mass, radius, orbital period, semi-major axis, eccentricity; and parent star parameters, including mass, radius, effective temperature, metallicity, and age. Filling out their distribution in this multidimensional space is certain to give us important information on the origin and evolution of exoplanetary systems. Here we report on the discovery by HATNet of its sixth transiting planet, HAT-P-6b, an inflated Jupiter-mass gas giant in an essentially circular orbit about an F dwarf star with slightly sub-solar metallicity.

2. PHOTOMETRIC DETECTION

The HATNet telescopes HAT-6 and HAT-9 (HATNet; Bakos et al. 2002, 2004) observed HATNet field G161, centered at $\alpha=00^{\rm h}32^{\rm m},~\delta=+37^{\circ}30',$ on a near-nightly basis from 2005 August 12 to 2005 December 16. We have gathered altogether 9550 5-min exposures, each yielding photometric measurements for approximately 35,000 stars with I<14 and about 10,000 stars with

¹ Harvard-Smithsonian Center for Astrophysics, Cambridge, MA, rnoyes@cfa.harvard.edu

² Hubble Fellow

³ Department of Astronomy, Eötvös Loránd University, Budapest, Hungary.

⁴ Konkoly Observatory, Budapest, Hungary

⁵ Department of Physics and Astronomy, San Francisco State University, San Francisco, CA
⁶ Department of Terrestrial Magnetism, Carnegie Institute of

⁶ Department of Terrestrial Magnetism, Carnegie Institute of Washington, DC

⁷ Department of Astronomy, University of California, Berkeley, CA

⁸ Tokyo Institute of Technology, Tokyo, Japan

⁹ Hungarian Astronomical Association, Budapest, Hungary

[†] Based in part on observations obtained at the W. M. Keck Observatory, which is operated by the University of California and the California Institute of Technology. Keck time has been in part granted by NASA (run N162Hr) and NOAO (run A285Hr).

better than 2% light curve rms. The field was observed in network mode, whereby at the end of its nightly observing sequence the HAT-6 telescope in Arizona handed off to the HAT-9 telescope in Hawaii, thus extending the duration of continuous observations. Following standard frame calibration procedures, astrometry was performed as described in Pál & Bakos (2006), and aperture photometry results were subjected to External Parameter Decorrelation (EPD, described briefly in Bakos et al. 2007a), and the Trend Filtering Algorithm (TFA; Kovács et al. 2005). We searched the light curves for box-shaped transit signals using the BLS algorithm of Kovács et al. (2002). A very significant periodic dip in intensity was detected in the $I \approx 10.6$ magnitude star GSC 03239-00992 (also known as 2MASS 23390581+4227575, with a depth of 9 mmag, a period of $P = 3.8529 \,\mathrm{days}$, and a duration of 3.1 hours.

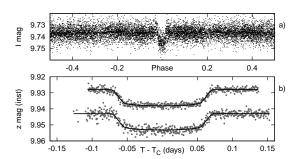


Fig. 1.— (a) Unbinned instrumental I-band discovery light curve of HAT-P-6 obtained with HATNet, folded with the period of P=3.852985 days. Superimposed (larger dots) is the same data binned to 1/200 in phase. (b) Unbinned instrumental Sloan z-band photometry collected with the KeplerCam at the FLWO 1.2 m telescope on 2006 October 26 (top curve) and again on UT 2007 September 4 (next curve); superimposed on both is our best-fit transit model curve (see text).

The HATNet discovery light curve is shown in Fig. 1a. As is shown in the following sections we deduce that the signal is due to the transit of a Jovian planet across the face of the star. Hereafter we refer to the star as HAT-P-6, and to the planetary companion as HAT-P-6b.

2 Noyes et al.

 $\begin{array}{c} {\rm TABLE\ 1} \\ {\rm Relative\ radial\ velocity\ measurements} \\ {\rm of\ HAT-P-6} \end{array}$

BJD (2,400,000+)	$\mathrm{RV}_{(ms^{-1})}$	$\sigma_{\rm RV} \ ({ m ms}^{-1})$
54022.70228 54023.78901 54085.81512 54130.72257 54247.11201 54248.08955 54249.08558 54250.12528 54251.08766	$\begin{array}{c} +74.01 \\ +47.70 \\ -3.70 \\ +62.40 \\ +67.25 \\ -110.02 \\ -94.78 \\ +66.22 \\ +56.10 \end{array}$	4.85 4.85 5.72 6.93 4.55 4.91 4.23 4.61 4.21
54258.11601 54279.09485 54286.12699 54319.11890 54336.87654 54337.86117	+103.71 -127.75 -18.23 $+32.41$ -112.33 -59.68	4.09 6.05 6.84 4.30 4.13 4.41

3. FOLLOW-UP OBSERVATIONS

HAT-P-6 was observed spectroscopically with the CfA Digital Speedometer (Latham 1992) at the FLWO 1.5 m Tillinghast reflector of the Fred L. Whipple Observatory (FLWO) in order to rule out the possibility that the observed drop in brightness is caused by a transiting low-mass stellar companion rather than a planet, as well as to characterize the rotation and surface gravity of the star. Seven spectra were obtained over an interval of 92 days. Radial velocities were obtained by cross-correlation and have a typical precision of $0.4\,\mathrm{km\,s^{-1}}$. They showed no variation within the uncertainties, ruling out a companion of stellar mass. The mean heliocentric radial velocity is $-22.7\pm0.5\,\mathrm{km\,s^{-1}}$.

Photometric follow-up of HAT-P-6 was then carried out in the Sloan z-band with KeplerCam (see e.g. Holman et al. 2007) on the FLWO 1.2 m telescope, on 2006 October 26. An astrometric solution between the individual frames and the 2MASS catalog was carried out using first order polynomials based on ~ 400 stars per frame. Aperture photometry was performed using a series of apertures in fixed positions around the 2MASSbased (x, y) pixel coordinates. We selected a frame taken near the meridian and used ~ 260 stars and their magnitudes as measured on this reference frame to transform all other frames to a common instrumental magnitude system. The aperture yielding the lowest scatter outside of transit was used in the subsequent analysis. The light curve was then de-correlated against trends using the out-of-transit sections and a dependence on hour angle (see Fig. 1b, upper curve).

A follow-up KeplerCam observation was recently obtained (2007 Sep 4), for the purpose of improving the photometric accuracy of the transit curve model, and also to determine the orbital period and mid-transit time with maximum accuracy. The data were treated identically to those for the 2006 October 26 transit; results are shown in the lower curve of Fig. 1b.

Following the first KeplerCam observation, high resolution spectroscopy was initiated with the HIRES instrument (Vogt et al. 1994) on the Keck I telescope, in order both to determine the stellar parameters more precisely and to characterize the radial velocity signal due to the companion. With a spectrometer slit of 0".86 the

resolving power is $\lambda/\Delta\lambda \approx 55{,}000$, and the wavelength coverage is $\sim 3800-8000$ Å. An iodine gas absorption cell was used to superimpose a dense forest of I₂ lines on the stellar spectrum and establish a highly accurate wavelength fiducial (see Marcy & Butler 1992). In total 15 exposures were obtained between 2006 October 14 and 2007 August 25 with the iodine cell, along with one without I₂ for use as a template. Relative radial velocities in the Solar System barycentric frame were derived as described by Butler et al. (1996), incorporating full modeling of the spatial and temporal variations of the instrumental profile. Data and their internal errors are listed in Table 1.

4. Analysis

We determined the parameters of the star, and of the transiting planet, from the combined photometric and spectroscopic data by the following procedure.

First, the iodine-free template spectrum from Keck was used for an initial determination of the atmospheric parameters of the star. Spectral synthesis modeling was carried out using the SME software (Valenti & Piskunov 1996), with wavelength ranges and atomic line data as described by Valenti & Fischer (2005). We obtained initial values as follows: effective temperature $T_{\rm eff}=6353\pm88K$, surface gravity $\log g_{\star}=3.84\pm0.12$, iron abundance [Fe/H] = -0.23 ± 0.08 , and projected rotational velocity $v\sin i=8.7\pm1.0\,{\rm km\,s^{-1}}$. The temperature and surface gravity correspond to an F8 dwarf. The uncertainties in SME-derived parameters quoted here and in the remainder of this discussion are twice the statistical uncertainties; this reflects our attempt, based on prior experience, to incorporate systematic errors.

Next, an initial modeling of the 2006 KeplerCam light curve was carried out using the formalism based on Mandel & Agol (2002), using the quadratic model for limb darkening without the assumption that the planet is small. The initial quadratic limb-darkening coefficients (namely, $\gamma_1 = 0.1452$ and $\gamma_2 = 0.3488$) were taken from the tables of Claret (2004) by interpolation to the abovementioned SME values. The period was initially fixed at the value given earlier from the HATNet photometry, and the orbit was assumed to be circular, based on the results from the radial velocity fit to be discussed below. The four adjustable parameters are the planet-to-star ratio of the radii (R_p/R_{\star}) , the normalized separation (a/R_{\star}) where a is the semi-major axis of the relative orbit, the normalized impact parameter ($b \equiv a \cos i/R_{\star}$), and the time of the center of the transit (T_c) . Both for the initial light curve fit and the further fits (see below) we used the Markov Chain Monte-Carlo (MCMC) method to find the best fit parameters (see, e.g. Ford 2004, for a comprehensive description). To estimate errors we used the method of refitting to synthetic data sets to determine their uncertainties and correlations. The synthetic data sets consist of the analytic (fitted) model plus Gaussian and red-noise, based on both white-noise and red-noise estimates of the residuals. The characteristics of the red noise component of the residuals were preserved by perturbing only the phase of their Fourier spectrum. We found that this method of error estimation is preferable to direct estimation using the MCMC method, since it is not sensitive to the number of out-of-transit points used. We also note that instead of a/R_{\star} and b, we used

Parameter	Value	Source
T_{eff} (K)	6570 ± 80	SME^a
[Fe/H]	-0.13 ± 0.08	SME
$\log g_{\star} \ (\mathrm{cgs}) \dots$	4.22 ± 0.03	$Y^2+LC+SME^b$
$v\sin i (\mathrm{km}\mathrm{s}^{-1}) \dots$	8.7 ± 1.0	SME
$M_{\star} (M_{\odot}) \ldots \ldots$	1.29 ± 0.06	$Y^2+LC+SME$
$R_{\star} (R_{\odot}) \dots$	1.46 ± 0.06	$Y^2+LC+SME$
L_{\star} (L_{\odot})	$3.57^{+0.52}_{-0.43}$	$Y^2+LC+SME$
$M_V \text{ (mag)}$	3.36 ± 0.16	$Y^2+LC+SME$
Age (Gyr)	$2.3^{+0.5}_{-0.7}$	$Y^2+LC+SME$
Distance (pc)	260 ± 20	$Y^2+LC+SME$

^aSME = Package for analysis of high-resolution spectra Valenti & Piskunov (1996).

the parameters ζ/R_{\star} and b^2 for the fit, where ζ is an auxiliary variable with dimensions of velocity, defined by $\zeta \equiv 2\pi a/\left(P\sqrt{1-b^2}\right)$. These parameters have been chosen to eliminate the correlation between a/R_{\star} and b^2 (see also Bakos et al. 2007b).

Next, we used the values of $T_{\rm eff}$ and [Fe/H] from the initial SME analysis, together with the initial value of a/R_{\star} from the Mandel-Agol fit, to estimate the stellar properties from comparison with the Yonsei-Yale (Y²) stellar evolution models by Yi et al. (2001). The value of a/R_{\star} is closely related to the stellar density, and is thus a proxy for luminosity (L_{\star}) . As described by Sozzetti et al. (2007), a/R_{\star} is typically a better constraint on L_{\star} than the spectroscopic value of $\log g_{\star}$, which has a relatively subtle effect on the line profiles and whose determination is therefore more susceptible to systematic errors. Following Sozzetti et al. (2007) we determined the range of stellar masses and radii that are consistent with the SME-determined values of $T_{\rm eff}$, [Fe/H], and a/R_{\star} derived from the light curve. We obtained $M_{\star} = 1.19^{+0.12}_{-0.10} M_{\odot}$ and $R_{\star} = 1.45^{+0.21}_{-0.17} R_{\odot}$. The resultant surface gravity, $\log g_{\star} = 4.19^{+0.08}_{-0.10}$, was significantly larger than the initial SME-derived value discussed above. We fixed $\log g_{\star}$ at this new, more accurate value, and repeated the SME analysis. Fixing surface gravity slightly affects the solution for other parameters such as [Fe/H] and other individual element abundances as well as $v \sin i$. The correlations between these free parameters in turn affect the final solution for effective temperature, causing it to change by about twice its original uncertainty. The resulting values from this iteration are $T_{\rm eff} = 6570 \pm 80 \, {\rm K}$, $[\text{Fe/H}] = -0.13 \pm 0.08$, and $v \sin i = 8.2 \pm 1.0 \,\text{km s}^{-1}$.

We then performed a second iteration of the above steps using the new values of $T_{\rm eff}$, $\log g_{\star}$, and [Fe/H], as well as correspondingly changed limb darkening coefficients: $\gamma_1 = 0.1211$ and $\gamma_2 = 0.3646$. This iteration also incorporated both the 2006 and 2007 KeplerCam light curves (Fig. 1b) into a single fit, which yielded the times of each transit center T_{c1} and T_{c2} , as well as the shape parameters a/R_{\star} , R_p/R_{\star} , and b, which we assumed to be the same for both of the transit events.

Finally, using the new values of a/R_{\star} , $T_{\rm eff}$, and [Fe/H] together with the Y² evolutionary models discussed above, we re-determined the stellar parameters. Table 2 summarizes these, which include a further refined deter-

TABLE 3
SPECTROSCOPIC AND LIGHT CURVE SOLUTIONS FOR HAT-P-6, AND INFERRED PLANET PARAMETERS

Parameter	Value
Light curve parameters	
$\begin{array}{l} P \; ({\rm days}) \; \\ T_c \; ({\rm HJD-2,400,000}) \; \\ T_{14} \; ({\rm days})^{\rm a} \; \\ T_{12} = T_{34} \; ({\rm days})^{\rm a} \; \\ a/R_{\star} \; \\ k_p/R_{\star} \; \\ b \equiv a \cos i/R_{\star} \; \\ i \; ({\rm deg}) \; \\ \zeta \; (R_{\star}/{\rm day}) \; \end{array}$	$\begin{array}{c} 3.852985 \pm 0.000005 \\ 54,035.67575 \pm 0.00028 \\ 0.1461 \pm 0.0017 \\ 0.0188 \pm 0.0011 \\ 7.69 \pm 0.22 \\ 0.09338 \pm 0.00053 \\ 0.602 \pm 0.030 \\ 85^{\circ}51 \pm 0^{\circ}35 \\ 15.696 \pm 0.086 \end{array}$
Spectroscopic parameters	
$K \text{ (m s}^{-1}) \dots $ $\gamma \text{ (km s}^{-1}) \dots $ $e \dots \dots \dots$	115.5 ± 4.2 -22.7 ± 0.5 0 (adopted)
Planet parameters	
$M_p (M_J) \dots$ $R_p (R_J) \dots$ $\rho_p (g \operatorname{cm}^{-3}) \dots$ $a (\operatorname{AU}) \dots$ $g_p (\operatorname{m} \operatorname{s}^{-2}) \dots$	$\begin{array}{c} 1.057 \pm 0.119 \\ 1.330 \pm 0.061 \\ 0.558 \pm 0.047 \\ 0.05235 \pm 0.00087 \\ 14.8 \pm 1.0 \end{array}$

^a T_{14} : total transit duration, time between first to last contact; $T_{12} = T_{34}$: ingress/egress time, time between first and second, or third and fourth contact.

mination of $\log g_{\star} = 4.217^{+0.029}_{-0.027}$. This value is the same as the one in the previous iteration to within uncertainties, so we stopped the iteration at this point.

From the value of $v \sin i$ and the stellar radius R_{\star} , and assuming an inclination of the rotational equator of approximately 90 deg (that is, similar to the inclination of the planetary orbital plane), we estimate the stellar rotation period to be about 9 days. We have searched the HATNet light curve (after elimination of data during transits) for periodicities between 6 and 12 days, such as might be produced by significant spots or other stellar activity, and found no evidence for this.

An independent estimate of the age was obtained from the Ca⁺ H and K line emission strength, measured from the mean of 14 Keck spectra: $\log R_{HK} = -4.81$, leading to an age of 2.8 Gy (based on Noyes et al. 1984), consistent with the evolutionary track age. The luminosity and $T_{\rm eff}$, imply an absolute visual magnitude $M_V = 3.36 \pm 0.16$ mag. Combined with the apparent visual magnitude ($V = 10.440 \pm 0.036$; Droege et al. 2006; Hog et al. 2000), this yields a distance of 260 ± 20 pc, ignoring extinction. For reference, the final values for the stellar parameters listed above are given in Table 2.

Setting the difference between the transit centers of the two KeplerCam light curves, $T_{c2} - T_{c1}$, to 81 orbital periods, we obtain a more accurate value for the period: $P = 3.852985 \pm 0.000005$ days. This value, and the reference epoch of mid-transit, $T_c \equiv T_{c1} = 2,454,035.67575 \pm 0.00028$, are given in Table 3. Also given in Table 3 are the final fitted light curve parameters a/R_{\star} , R_p/R_{\star} , b, i (orbital inclination), and the radius of the planet, $R_p = 1.330 \pm 0.061 R_{\rm J}$, as determined from R_{\star} and R_p/R_{\star} . The modeled z-band transit light curve is shown as a solid line superimposed on the data points in Fig. 1b.

The Keck radial velocity data were initially fit with a Keplerian model with period and epoch constrained to

^bY²+LC+SME = Yale-Yonsei isochrones (Yi et al. 2001), light curve parameters, and SME results.

4 Noyes et al.

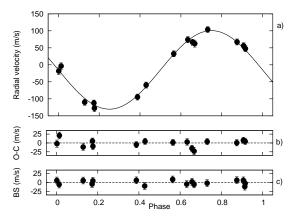


FIG. 2.— (a) Radial-velocity measurements from Keck for HAT-P-6, along with an orbital fit, shown as a function of orbital phase. The center-of-mass velocity has been subtracted. (b) Phased residuals after subtracting off the orbital fit. The rms variation of the residuals is about $8.6 \,\mathrm{m\,s^{-1}}$. (c) Bisector spans (BS) for the 16 Keck spectra plus the single template spectrum, computed as described in the text. The mean value has been subtracted. Vertical scale for all three panels is the same.

the value determined from the photometry (§2) and no constraint on eccentricity. We found an eccentricity of $e=0.046\pm0.031$, not significantly different from zero. Therefore the data were re-fit with a circular orbit, in which both the period P and the mid-transit time T_c were held fixed at their values from the light curve analysis (Table 3). The solution fits the data well; see Fig. 2a. No long-term trends are seen in the residuals.

In order to get a reduced chi-square value near unity for the fit, it was necessary to add an additional random noise component with amplitude 8.6 m s⁻¹ in quadrature to the internal errors. This is essentially identical to the 8.7 m s⁻¹ radial velocity "jitter" expected to arise from stellar surface activity, based on the above-mentioned strength of the emission cores of the Ca⁺ H and K lines, $\log R'_{HK} = -4.81$ (Wright 2005). The parameters of the resulting final fit are not significantly changed by the inclusion of this jitter, and are listed in Table 3.

Following Torres et al. (2007), we explored the possibility that the measured radial velocities are not real, but instead due to distortions in the spectral line profiles due to contamination from a nearby unresolved eclipsing binary. In that case the "bisector span" of the average spectral line should vary periodically with amplitude and phase similar to the measured velocities themselves (Queloz et al. 2001; Mandushev et al. 2005). Instead, we detect no variation in excess of the measurement uncertainties (see Fig. 2, bottom panel). We conclude that the velocity variations are real and that the star is orbited by a Jovian planet.

Combined with the results from the light curve and radial velocity modeling, the above stellar parameters yield a planet mass of $M_p = 1.06 \pm 0.12 \, M_{\rm J}$. The surface gravity, $g_p = 14.8 \pm 1.0 \, {\rm m \, s^{-1}}$, was obtained from the light curve and radial velocity fits (see Southworth et al. 2007). The mean density and its uncertainty, $\rho_p = 0.558 \pm 0.047 \, {\rm g \, cm^{-3}}$, follow from the absolute radius of the planet. All planet parameters are listed in Table 3.

5. DISCUSSION

 $\mathrm{HAT} ext{-}\mathrm{P} ext{-}\mathrm{6b}$, with radius $1.33\,R_\mathrm{J}$, is similar in size to five low density "inflated" planets tabulated by Kovács

et al. (2007) (i.e. WASP-1b, HAT-P-4b, HD 209458b, TrES-4, and HAT-P-1b). However, its mass of $1.06 M_{\rm I}$ is greater than the mass of any of these, and hence it has a larger mean density and surface gravity. For a planet of its mass, age of 2.3 Gy, and stellar flux F_p at the planet given by $F_p = L_{\star}/(4\pi a^2)$, models of Burrows et al. (2007) predict a radius of about 1.21 $R_{\rm J}$, assuming that the planet has no heavy-element core. The metallicity of HAT-P-6, $[Fe/H] = -0.13\pm0.08$, is among the smallest of known transiting planet host stars. If we assume that the bulk composition of HAT-P-6b tracks the metallicity of its host star, the size of its heavy-element core should be small, but not vanishingly so. Thus the predicted radius from Burrows et al. (2007) is comparable to, but perhaps slightly higher, than one might expect for HAT-P-6b. However, the actual radius found here, $R_p = 1.330 \pm$ 0.061, lies above the predicted value by about 2σ , so it appears to be somewhat inflated relative to that model.

Hansen & Barman (2007) proposed that hot jupiters can be placed into two classes based on their equilibrium temperature and Safronov number Θ , where $\Theta \equiv$ $(a/R_p) \times (M_p/M_{\star})$ is the ratio of the escape velocity from the surface of the planet to the orbital velocity. When Safronov number is plotted versus equilibrium temperature, transiting hot jupiters seem to fall into two groups, with an absence of objects between. However, the Safronov number for HAT-P-6b is 0.064±0.004; along with HAT-P-5b (Bakos et al. 2007b) with Safronov number 0.059 ± 0.005 , these two planets appear to fall between the two groups in such a plot. Hansen & Barman also noted a difference in the relation between planet mass and equilibrium temperature for planets of the two classes, but HAT-P-6b and HAT-P-5b appear to fall between the two classes in this respect as well. It would seem that discovery and characterization of a large number of additional transiting exoplanets may be necessary to establish unambiguously whether there is a bimodal distribution of hot jupiter planets according to their Safronov number.

Operation of the HATNet project is funded in part by NASA grant NNG04GN74G. We acknowledge partial support also from the Kepler Mission under NASA Cooperative Agreement NCC2-1390 (D.W.L., PI). G.T. acknowledges partial support from NASA under grant NNG04LG89G, and work by G.A.B. was supported by NASA through HST-HF-01170.01-A Hubble Fellowship Grant. G.K. and A.P. thank the Hungarian Scientific Research Foundation (OTKA) for support through grant K-60750. A.P. would like to thank the hospitality of the CfA, where this work has been partially carried out, and acknowledge support from the Doctoral Scholarship of Eötvös University. This research has made use of Keck telescope time granted through NASA and NOAO, of the VizieR service (Ochsenbein et al. 2000) operated at CDS, Strasbourg, France, of NASA's Astrophysics Data System Abstract Service, and of the 2MASS Catalog.

REFERENCES

Bakos, G. Á., Lázár, J., Papp, I., Sári, P., & Green, E. M. 2002, PASP, 114, 974

Bakos, G. Á., Noyes, R. W., Kovács, G., Stanek, K. Z., Sasselov, D. D., & Domsa, I. 2004, PASP, 116, 266

Bakos, G. Á., et al. 2007a, ApJ, in press (arXiv:0705.0126)

Bakos, G. Á., et al. 2007b, ApJ, submitted (arXiv:0710.1841)

Burrows, A., Hubeny, I., Budaj, J., & Hubbard, W. B. 2007, ApJ, 661, 502

Butler, R. P., Marcy, G. W., Williams, E. et al. 1996, PASP, 108, 500

Claret, A. 2004, A&A, 428, 1001

Droege, T. F., Richmond, M. W., & Sallman, M. 2006, PASP, 118, 1666

Ford, E. B. 2004, AJ, 129, 1706

Hansen, B., & Barman, T. 2007, preprint (arXiv:0706.3052v1)

Hog, E. et al. 2000, A&A, 355, 27

Holman, M. J. et al. 2007, ApJ, in press (arXiv:0704.2907)

Kovács, G., Zucker, S., & Mazeh, T. 2002, A&A, 391, 369

Kovács, G., Bakos, G. Á., & Noyes, R. W. 2005, MNRAS, 356, 557 Kovács et al. 2007, ApJ, in press (arXiv:0710.0602)

Latham, D. W. 1992, in IAU Coll. 135, Complementary Approaches to Double and Multiple Star Research, ASP Con535f. Ser. 32, eds. H. A. McAlister & W. I. Hartkopf (San Francisco: ASP), 110 Mandel, K., & Agol, E. 2002, ApJ, 580, L171

Mandushev, G., et al. 2005, ApJ, 621, 1061
Marcy, G. W., & Butler, B. P. 1992, PASP, 10.

Marcy, G. W., & Butler, R. P. 1992, PASP, 104, 270

Noyes, R. W., Hartmann, L. W., Baliunas, S. L., Duncan, D. K., & Vaughan, A. H. 1984, ApJ, 279, 763

Ochsenbein, F., Bauer, P., & Marcout, J. 2000, A&AS, 143, 23

Pál, A., & Bakos, G. Á. 2006, PASP, 118, 1474

Queloz, D., et al. 2001, A&A, 379, 279

Southworth, J., Wheatley, P. J., & Sams, G. 2007, MNRAS, in press (arXiv:0704.1570)

Sozzetti, A. et al. 2007, ÁpJ, 664, 1190

Torres, G., Bakos, G. Á, Kovacs, G. et al. 2007, ApJ, 666, 121

Valenti, J. A., & Fischer, D. A. 2005, ApJS, 159, 141

Valenti, J. A., & Piskunov, N. 1996, A&AS, 118, 595

Vogt, S. S. et al. 1994, Proc. SPIE, 2198, 362 Wright, J. T. 2005, PASP, 117, 657

Yi, S. K. et al. 2001, ApJS, 136, 417